

# Spin-dependent tunneling in metal-insulator-narrow gap semiconductor structures in a magnetic field

G.M.Minkov, O.E.Rut, and A.V.Germanenko

*Institute of Physics and Applied Mathematics, Ural University, Ekaterinburg 620083, Russia*

(October 6, 2018)

## Abstract

We present results of tunneling studies of p-Hg<sub>1-x</sub>Cd<sub>x</sub>Te-oxide-Al structures with  $0.165 < x < 0.2$  in a magnetic field up to 6 T. The tunneling conductivity oscillations resulting from the Landau quantization of the energy spectrum in the semiconductor volume are investigated. Under an in-plane magnetic field the amplitudes of tunneling conductivity maxima connected with the tunneling into  $a$  and  $b$  spin sublevels are found to differ substantially from one another, and the amplitude ratio varying from structure to structure. To understand the cause of this behavior, the tunneling conductivity for this magnetic field orientation is calculated taking into consideration the multi-band energy spectrum. It is shown that the contributions of the different spin-sublevels to the tunneling conductivity are dissimilar and the relationship between them depends strongly on the value of surface potential.

PACS number(s): 73.20.At, 73.40Gk, 73.40Qv

Typeset using REVTeX

## I. INTRODUCTION

The electron tunneling in metal – insulator – semiconductor (MIS) structures is a useful tool for studying the energy spectrum of two- and three-dimensional states, the interaction of carriers with the semiconductor-insulator boundary, the interaction with elementary excitations such as optical phonons, magnons, etc. [1] The tunneling in MIS structures based on wide-gap semiconductors, for example GaAs has been studied in detail. [2–11] In these semiconductors the electron effective  $g$ -factor is small and spin-dependent effects in tunneling do not manifest themselves. The opposite situation is observed in HgTe-type semiconductors with an inverted energy spectrum, where the electrons are the carriers of the fourfold degenerate (at  $k = 0$ ) band. The difference of contributions by different electron spin states to various phenomena for such materials was discussed by a number of authors. [12,13] It has been found experimentally that with the magnetic field parallel to the current, the amplitudes of Shubnikov-de-Haas oscillations connected with the different spin states differ largely. [12] An analogous difference in tunneling conductivity in structures based on inverted-spectrum semiconductors has been observed with magnetic field perpendicular to the normal to the plane of a tunneling structure ( $B \perp n$ ). [13] With this magnetic field orientation, the energy of the states depends not only on the quantum number,  $n$ , and the quasimomentum in the direction of the magnetic field,  $k_B$ , but also oscillation center – boundary distance,  $x_0$ , and this  $x_0$  dependence of the energy is essential for oscillation amplitudes of the tunneling conductivity in the magnetic field. It is well known that for a twofold degenerate parabolic band the energy of an electron increases monotonically with decreasing  $x_0$ . This  $E$ - $x_0$  relation is the same for both spin states. Consequently, the contributions to the tunneling conductivity, that come from tunneling into different spin states, should be close in magnitude in MIS structures based on such materials. In terms of the one-band energy spectrum model, magnetotunneling under an in-plane magnetic field was considered in Refs. [8–11]. In semiconductors with a complex spectrum, the behavior of the different spin states near the boundary may differ significantly and it should lead to a distinction in

tunneling into different spin states. Thus the behavior of the Landau levels in the vicinity of the boundary in the semiconductors with the energy spectrum described by the Dirac Hamiltonian was calculated in Ref. [14]. It was shown that in a symmetric band-inverted junction the Landau eigenenergies vary nonmonotonically with the orbit center – structure interface distance and this behavior varies for different spin states. The same problem was considered also for semiconductors with the inverted spectrum, described by the Luttinger Hamiltonian. [15] The behavior of the Landau levels near the boundary is different for different spin states in this case, too, and this fact was drawn on to explain the significant difference of the tunneling conductivity oscillation amplitudes associated with tunneling into different spin states in inverted semiconductor p-Hg<sub>1-x</sub>Cd<sub>x</sub>Te-insulator-metal tunneling structures at  $B \perp n$ . The fact that the electrons in inverted semiconductors were the carriers of the fourfold degenerate  $\Gamma_8$  band was essential to the explanation of the observed peculiarities.

Surprisingly, the similar peculiarities of the tunneling conductivity into different spin states at  $B \perp n$  are observed for some tunneling structures based on narrow-gap semiconductors, where the electrons are the carriers of the twofold degenerate  $\Gamma_6$  band. However, the ratio of the tunneling conductivity oscillation amplitudes associated with tunneling into different spin states varies widely for various tunnel structures. One possibility is that the surface potential at the semiconductor-insulator boundary is different in these tunneling structures. Such peculiarities of the tunneling into different spin states are the subject of the present paper.

The article is organized as follows. Section II presents and analyzes an experimental data for tunneling conductivity oscillations with various magnetic field orientations. Section III is devoted to the calculation of the behavior of the Landau levels near the surface of a Kane spectrum semiconductor. The basic equations and formalism are spelled out. Results of the calculation of tunneling conductivity oscillations and a comparison with experimental data are presented in Section IV.

## II. EXPERIMENTAL RESULTS

We have investigated the tunneling conductivity  $\sigma_d = dj/dV$  and its derivative  $d\sigma_d/dV$  as functions of bias  $V$  and magnetic field in p-Hg<sub>1-x</sub>Cd<sub>x</sub>Te-oxide-Al ( $0.165 < x < 0.21$ ) structures with  $10 < E_g < 100$  meV in magnetic fields up to 6 T at a temperature of 4.2 K. Tunnel structures were fabricated on single-crystal p-Hg<sub>1-x</sub>Cd<sub>x</sub>Te with uncompensated acceptor concentration  $N_A - N_D = (0.8 - 2) \times 10^{18}$  cm<sup>-3</sup>. The doping level was determined from an analysis of galvanomagnetic phenomena in the temperature range 4.2 - 80 K. The procedure for the fabrication of tunneling structures was described in our previous papers. [16,17] The resistance of our structures was 0.01 - 1 kOhm. Several tunnel structures prepared on each sample were investigated.

The energy diagram of the tunneling contact is shown in Fig. 1. The bias shifts the Fermi level of the metal relative to that of the semiconductor ( $E_F$ ) and the tunneling conductivity is proportional to the density of states in the semiconductor at energy  $E = E_F + eV$ . The magnetic field quantizes the energy spectrum of the semiconductor and the tunneling conductivity becomes an oscillatory function of magnetic field and bias. Typical oscillation pictures of the tunneling conductivity in a magnetic field at a fixed bias for two different structures are shown in Fig.2. It is seen that (i) for both structures the oscillation maxima are split, and at  $B \parallel n$  the amplitudes of the components are comparable in magnitude; (ii) the amplitudes of the maxima and magnetic field positions exhibit a rather complicated behavior in tilted magnetic field; (iii) at  $B \perp n$  the ratio of the amplitudes of the components are close in magnitude for structure I and they differ significantly for structure II, so that high-field components are hard to resolve at this magnetic field orientation. Similar peculiarities of oscillation maxima amplitudes are observed in the bias dependences of  $dj/dV$  at a fixed magnetic field (Fig. 3).

A Fourier analysis of the oscillations shows that the  $\sigma_d$  vs  $B^{-1}$  curves have two fundamental fields,  $B_1$  and  $B_2 = 2B_1$ . The values of fundamental fields do not vary with angle between  $B$  and  $n$ , only the amplitude of Fourier component  $B_2$  decreases when  $\Theta \rightarrow 90^\circ$  so

that it practically disappears for structure II. Thus, this behavior of the oscillation provides evidence that the tunneling conductivity oscillations for both structures are due to tunneling into bulk Landau levels, splitting of the oscillation maxima corresponds to the spin splitting of the Landau levels, and the probability of tunneling into spin-up and spin-down states for structure II is remarkably different at  $B \perp n$ .

The fundamental field  $B_1$  at bias  $V$  is determined by the value of quasimomentum at the energy  $E = E_F + eV$ ,  $B_1^{-1} = 2e/c\hbar k^2$ , so that measurements at various biases make it possible to obtain the dispersion law  $E(k)$  for a wide energy range. [18,19] For the structures investigated, the experimental data are in good agreement with the  $E(k)$  curve calculated in terms of the Kane model with parameters  $P = 8.2 \times 10^{-8}$  eV cm,  $E_g = 80$  meV,  $\Delta = \infty$ .

It is well known that the phenomena occurring in a tilted magnetic field are a very complicated problem. We will therefore restrict our attention to the results at  $B \parallel n$  and  $B \perp n$ , namely, the ratio between the oscillation amplitudes for tunneling into different spin states and the relationship of this ratio to the structure parameters.

Let us consider the tunneling current and tunneling conductivity at  $B \parallel n \parallel Ox$  and  $B \perp n \parallel Ox$ . For a metal-insulator-semiconductor structure, the Fermi energy of the metal is much greater than that of the semiconductor; therefore, upon summation over all metal states, the tunneling current for a structure with low barrier transparency can be written in the form

$$j(V) \propto D \sum_s (\hat{v}\Psi)_{x=0}^2 \quad (1)$$

Here  $D$  is the barrier transparency,  $\hat{v}$ ,  $\Psi$  are the electron velocity operator and the wave function in the semiconductor, and  $x = 0$  is the coordinate of the boundary. The summation runs over all states in the semiconductor, from energy  $E_F$  to  $E_F + eV$ .

In a magnetic field, the semiconductor's states are defined by three quantum numbers: Landau level number  $n$ , oscillator center position, and the quasimomentum component in the direction of the magnetic field. At  $B \parallel n \parallel Ox$  ( $B = B_x$ ) the quantity  $(\hat{v}_x \Psi_n)^2$  depends on  $k_x$  only, and going to integration over energy we obtain

$$\begin{aligned}
j(V) &\propto D \sum_n \int (\hat{v}\Psi_n)_{x=0}^2 dk_x \\
&= D \sum_n \int_{E_F}^{E_F+eV} (\hat{v}\Psi_n)_{x=0}^2 \frac{dk_x}{dE} dE
\end{aligned} \tag{2}$$

$$\sigma_d(V) \equiv \frac{dj}{dV} \propto D (\hat{v}\Psi_n)_{x=0}^2 \left. \frac{dk_x}{dE} \right|_{E=E_F+eV} \tag{3}$$

In the magnetic field  $B \perp n \parallel Ox$ , the Landau eigenenergies are a function of the orbit center-barrier distance  $x_0$  and  $k_B$ , so the square of the velocity at the boundary is also a function of  $x_0$  and  $k_B$ ,

$$\begin{aligned}
j(V) &\propto D \sum_n \int \int (\hat{v}\Psi_n)_{x=0}^2 dx_0 dk_B \\
&= D \sum_n \int \int (\hat{v}\Psi_n)_{x=0}^2 dk_B \left( \frac{dE}{dx_0} \right)^{-1} dE
\end{aligned} \tag{4}$$

$$\sigma_d(V) \propto \int_0^{k_B^{max}} (\hat{v}\Psi_n)_{x=0}^2 \left( \frac{dE}{dx_0} \right)^{-1} dk_B \Big|_{E=E_F+eV} \tag{5}$$

Thus, to calculate the tunneling conductivity at  $B \perp n$ , one needs to calculate the distance dependencies of the velocity and energy near the boundary. This problem for a semiconductor with a Kane spectrum is considered in the next section.

### III. THE LANDAU LEVELS NEAR THE BOUNDARY AT $B \perp n$

To calculate the behavior of the Landau levels near the boundary at  $B \perp n$  and the tunneling current for this magnetic field orientation, let us consider an insulator-semiconductor structure with an abrupt interface (Fig. 4). We assume that the insulator has the same energy structure as the semiconductor with the same momentum matrix element  $P$  but with an energy gap value much greater than that for a semiconductor. [20] The parameters  $D_c$ , and  $D_v$  are the conduction and valence band offsets, respectively. For such a structure we can solve the Schrödinger equation for  $x < 0$  (i.e., for an insulator) and  $x > 0$  (i.e., for a semiconductor) independently. Matching these solutions at  $x = 0$  in the required way, we find the solution for entire structure.

We use the Kane energy spectrum model for a semiconductor and an insulator. The interaction with remote and spin-orbit split  $\Gamma_7$  bands is neglected. We choose the direction  $x$  to be normal to the interface and  $z$  to be aligned with the magnetic field ( $B = (0, 0, B)$ ,  $B \perp n$ ). The electromagnetic vector potential  $A$  is chosen as  $A = (0, B(x - x_0), 0)$ . In this case the components of the momentum operator are  $\hat{k}_x = -i\frac{\partial}{\partial x}$ ,  $\hat{k}_y = -L^{-2}(x - x_0)$ ,  $\hat{k}_z = k_z = k_B$ . Here  $L = \sqrt{\hbar c/eB}$  is the magnetic length. To start with we wish to consider this problem for  $k_z = k_B = 0$ . In this case the Schrödinger equation  $\hat{H}\Psi = E\Psi$  splits up into two independent equations corresponding to the Landau spin sublevels, designated as  $a$ - and  $b$ -sets. For the  $a$ -set these equations read as

$$\hat{H}^a\Psi^a = E\Psi^a, \quad (6)$$

where

$$\hat{H}^a = \begin{pmatrix} E_g & -\frac{i}{\sqrt{6}}\frac{P}{L}\left(\frac{\partial}{\partial\xi} + (\xi - \xi_0)\right) & -\frac{i}{\sqrt{2}}\frac{P}{L}\left(\frac{\partial}{\partial\xi} - (\xi - \xi_0)\right) \\ -\frac{i}{\sqrt{6}}\frac{P}{L}\left(\frac{\partial}{\partial\xi} - (\xi - \xi_0)\right) & 0 & 0 \\ -\frac{i}{\sqrt{2}}\frac{P}{L}\left(\frac{\partial}{\partial\xi} + (\xi - \xi_0)\right) & 0 & 0 \end{pmatrix},$$

and for the  $b$ -set,

$$\hat{H}^b\Psi^b = E\Psi^b, \quad (7)$$

where

$$\hat{H}^b = \begin{pmatrix} E_g & \frac{i}{\sqrt{2}}\frac{P}{L}\left(\frac{\partial}{\partial\xi} + (\xi - \xi_0)\right) & \frac{i}{\sqrt{6}}\frac{P}{L}\left(\frac{\partial}{\partial\xi} - (\xi - \xi_0)\right) \\ \frac{i}{\sqrt{2}}\frac{P}{L}\left(\frac{\partial}{\partial\xi} - (\xi - \xi_0)\right) & 0 & 0 \\ \frac{i}{\sqrt{6}}\frac{P}{L}\left(\frac{\partial}{\partial\xi} + (\xi - \xi_0)\right) & 0 & 0 \end{pmatrix}.$$

Here  $\xi = x/L$ , and  $\xi_0 = x_0/L$  are dimensionless coordinates, energies  $E$  and  $E_g$  are measured from the top of the semiconductor valence band. We seek solutions of (6) and (7) in the form

$$\Psi^\pm = \begin{pmatrix} c_1 u^\pm (a_1, (\xi - \xi_0)^2) \\ c_2 u^\pm (a_2, (\xi - \xi_0)^2) \\ c_3 u^\pm (a_3, (\xi - \xi_0)^2) \end{pmatrix} e^{-\frac{(\xi - \xi_0)^2}{2}} \quad (8)$$

where

$$u^\pm(a, x^2) = \frac{\sqrt{\pi}}{\Gamma(p + \frac{1}{2})} M(a, \frac{1}{2}, x^2) \pm \frac{2\sqrt{\pi}}{\Gamma(p)} x M(a + \frac{1}{2}, \frac{3}{2}, x^2),$$

and  $M(a, b, y)$  is a confluent hypergeometric function. [21] Using the properties of the confluent hypergeometric function, one can write the particular solutions for the  $a$ -set

$$\Psi_a^\pm = \begin{pmatrix} ELP^{-1}u^\pm(a, (\xi - \xi_0)^2) \\ i\sqrt{\frac{2}{3}}u^\pm(a - \frac{1}{2}, (\xi - \xi_0)^2) \\ i\sqrt{2}au^\pm(a + \frac{1}{2}, (\xi - \xi_0)^2) \end{pmatrix} e^{-\frac{(\xi - \xi_0)^2}{2}}, \quad (9)$$

where

$$a = \frac{3}{8} \left( \left( \frac{L}{P} \right)^2 E(E_g - E) + \frac{1}{3} \right)$$

and for the  $b$ -set,

$$\Psi_b^\pm = \begin{pmatrix} ELP^{-1}u^\pm(a, (\xi - \xi_0)^2) \\ -i\sqrt{2}u^\pm(a - \frac{1}{2}, (\xi - \xi_0)^2) \\ -i\sqrt{\frac{2}{3}}au^\pm(a + \frac{1}{2}, (\xi - \xi_0)^2) \end{pmatrix} e^{-\frac{(\xi - \xi_0)^2}{2}}, \quad (10)$$

where

$$a = \frac{3}{8} \left( \left( \frac{L}{P} \right)^2 E(E_g - E) + 1 \right).$$

The solutions for the insulator that correspond to the same energy as the solution for semiconductor are given by (9), (10), where  $E$  and  $E_g$  are changed to  $E + D_v$  and  $E_g + D_c + D_v$ , respectively.

The general solution for  $x > 0$  ( $R$ ) and  $x < 0$  ( $L$ ) for the  $a$ -set is

$$\Psi_a^{R,L}(x) = \begin{bmatrix} \psi_a^1(x) \\ \psi_a^2(x) \\ \psi_a^3(x) \end{bmatrix}_{R,L} = A^{R,L} [\Psi_a^+]_{R,L} + B^{R,L} [\Psi_a^-]_{R,L} \quad (11)$$



The general solution for the  $b$ -set is similar in form. The quantity  $\Psi^R$  has to converge at  $x \rightarrow +\infty$  and  $\Psi^L$  has to converge at  $x \rightarrow -\infty$ , so we must set  $A^R = B^L = 0$ . Matching conditions are obtained by integrating the Schrödinger equation across the boundary. For the  $a$ -set these conditions are:

$$\left[\psi_a^1(0)\right]_L = \left[\psi_a^1(0)\right]_R \quad (12a)$$

$$\left[\psi_a^2(0) + \sqrt{3}\psi_a^3(0)\right]_L = \left[\psi_a^2(0) + \sqrt{3}\psi_a^3(0)\right]_R \quad (12b)$$

and for the  $b$ -set,

$$\left[\psi_b^1(0)\right]_L = \left[\psi_b^1(0)\right]_R \quad (13a)$$

$$\left[\sqrt{3}\psi_b^2(0) + \psi_b^3(0)\right]_L = \left[\sqrt{3}\psi_b^2(0) + \psi_b^3(0)\right]_R \quad (13b)$$

These matching conditions give the secular equation for calculating the  $x_0$  dependence of energy. This problem was solved numerically with parameters corresponding to the samples investigated ( $E_g = 80$  meV,  $P = 8.2 \times 10^{-8}$  eV cm) and  $D_c = 2$  eV,  $D_v = 1$  eV. [16] Such curves for the  $a$ - and  $b$ -sets are presented in Fig. 5 in dimensionless coordinates  $(x/L, E/\hbar\omega_n)$ , where  $\omega_n = eB/m_n c$ , and  $m_n$  is the electron effective mass at the conduction band bottom. A pronounced difference between the spin sublevels is seen. This is the result of the spin-orbit interaction with the boundary.

#### IV. DISCUSSION

It is evident from Eq.(5) that to calculate the tunneling conductivity, we need the  $x_0$  dependence of the velocity squared at the boundary. With the definition of the velocity operator  $\hat{v} = i/\hbar[Hx]$  we have calculated  $(\hat{v}\Psi)^2$  for the levels presented in Fig. 5, and as an illustration these results for sublevels  $a_1$ , and  $b_1$  are plotted in Fig. 6. In calculating the tunneling conductivity, we have assumed that the  $x_0$  dependencies of energy and  $(\hat{v}\Psi)^2$  have the same form at any  $k_B$  (Fig. 5, 6). In Fig. 7 we show the contributions that the

tunneling into different Landau sublevels makes to the tunneling conductivity as calculated from Eq.(5). Note that tunneling into  $b$ -levels is more effective in consequence of differences in the  $E$  vs  $x_0$  and  $(\hat{v}\Psi)^2$  vs  $x_0$  curves for  $a$  and  $b$  sublevels. The model discussed here has only two parameters,  $D_c$ , and  $D_v$ , and the results have only a weak dependence on these parameters. Finally, summing the contributions to the tunneling conductivity by the different Landau sublevels and subtracting the monotone component, we obtain the oscillatory part of the tunneling conductivity presented in Fig. 8. For comparison, we show in Fig. 8 also the oscillations of the tunneling conductivity of the same structure at  $B \parallel n$ , which are calculated in the same way as in Ref. [17]. It is seen that at  $B \parallel n$  the amplitudes of the tunneling maxima connected with tunneling into  $a$  and  $b$  sublevels are close in magnitude.

Inspection of the experimental and calculated results (Figs. 3, 8) shows that the relationship among the oscillation amplitudes at  $B \parallel n$  agree well with experimental data for both structures. Whereas at  $B \perp n$  the ratio of the  $a$ -maximum amplitude to the  $b$ -maximum amplitude is appreciably greater than the calculated value for structure I, but much less for structure II. One conceivable reason for this discrepancy is the presence of an attractive or a repulsive potential in the semiconductor near the semiconductor-insulator interface. In order to verify this assumption the above calculation was carried out for structures with a model potential which we suppose as a rectangular well (or a barrier) of width  $d$  and value  $U$ . In this case the wave functions in three regions,  $x < 0$ ,  $0 < x < d$  and  $x > d$ , have the same form (11). It is essential that for  $0 < x < d$  both terms in Eq.(11) should be taken into account. The requirement that the boundary conditions (12) and (13) be fulfilled at  $x = 0$  and at  $x = d$  gives a secular equation for calculating the  $x_0$  dependence of energy. The results of calculations for the surface well ( $eU = -70$  meV,  $d = 25$  Å) and the barrier ( $eU = 70$  meV,  $d = 25$  Å) are presented in Figs. 9, and 10. The parameters of the potential are so adjusted that the well cannot hold the 2D states. It is seen that the effect of the surface potential is different for the  $a$ - and  $b$ -sublevels. As a result, the ratio between amplitudes of tunneling conductivity maxima associated with tunneling into  $a$ - and  $b$ -sublevels is strongly dependent on the surface potential. For the repulsive potential the amplitudes

of  $a$ - and  $b$ -maxima can be close in magnitude (Fig. 10c), as is experimentally observed for structure I (Fig. 3a), while for a sufficiently large attractive potential only  $b$ -maxima are visible (Fig. 10a), as is experimentally observed for structure II (Fig. 3b). Note that for  $B \parallel n$ , the calculated and experimentally observed amplitudes of the tunneling conductivity maxima associated with tunneling into  $a$ - and  $b$ -sublevels are close in magnitude, for both the attractive and the repulsive potential.

Thus, the ratio of amplitudes of maxima due to tunneling into  $a$  and  $b$  sublevels at  $B \perp n$  depends on the surface potential and provides a way for estimating the value of the surface potential under conditions where the surface potential is small and cannot localize the 2D states.

As mentioned above (ii), the amplitudes of the maxima and the magnetic field positions in a tilted magnetic field exhibit a rather complicated behavior (Fig. 2). This is clearly seen for maxima observed in a high magnetic field. The positions of the maxima vary nonmonotonically with angle and with  $\Theta \simeq 50^\circ$  their amplitudes decrease drastically. Basically, the same behavior has been observed for all the structures investigated.

In addition, we would like to point out one further peculiarity of tunneling conductivity in a tilted magnetic field. It is most pronounced in bias dependencies of  $d\sigma_d/dV$  in the structures based on narrower-gap  $\text{Hg}_{1-x}\text{Cd}_x\text{Te}$  (Fig. 11). A fine structure of maxima associated with tunneling into  $b$ -sublevels arises with magnetic field orientations close to  $B \perp n$  ( $85^\circ > \Theta > 50^\circ$ ). All  $b$ -maxima have a similar fine structure. The calculations of the energy spectrum and tunneling in a tilted magnetic field are essential to understanding of peculiarities observed. To the authors' knowledge, such calculations for structures based on Kane semiconductors are not available.

## V. CONCLUSION

Tunneling conductivity oscillations in a magnetic field have been investigated for structures based on narrow-gap  $\text{Hg}_{1-x}\text{Cd}_x\text{Te}$ . These oscillations in the structure investigated are

shown to arise from tunneling into bulk Landau levels. Rather remarkably, at  $B \perp n$  the relationship of the amplitudes of the maxima associated with tunneling into different spin states varies significantly for the structures investigated, so that only tunneling into one-spin sublevels is observed in some structures.

To understand the causer of this distinction, we have calculated the behavior of the Landau levels near the surface and the tunneling conductivity oscillation at  $B \perp n$ . The relationship of the amplitudes of the maxima associated with tunneling into different spin states is shown to depend dramatically on the surface potential. Thus the investigations of the tunneling conductivity at  $B \perp n$  provide a way to estimate the value of the surface potential when this is small and cannot localize the 2D states.

## REFERENCES

- [1] E. L. Wolf, Sol. St. Phys. **30**, 1 (1975).
- [2] S. Ben Amor, J. J. L. Rascol, K. P. Martin, R. J. Higgins, R. C. Potter, and H. Hier, Phys. Rev. B **41**, 7860 (1990).
- [3] W. Demmerle, J. Stoliner, G. Berthold, E. Gornik, G. Weimann, and W. Schlapp, Phys. Rev. B **44**, 3090 (1991).
- [4] R. S. Ashori, J. A. Lebens, N. P. Bigelow, and R. H. Silsbee, Phys. Rev. B **48** 4616 (1993).
- [5] J. Smoliner, T. Suski, C. Gschlössl, W. Demmerle, G. Böhm, and G. Weimann, Phys. Rev. B **47** 3760 (1993).
- [6] A. R. Bonnefoi, D. H. Chow, and T. S. McGill, J. Appl. Phys. **32** 3836 (1987).
- [7] Timothy B. Boykin, R. E. Carnahan, and K. P. Martin, Phys. Rev. B **50** 15393 (1994).
- [8] L. Brey, G. Platero, and C. Tejedor, Phys. Rev. B **38** 9649 (1993).
- [9] L. Eaves, K. W. H. Stevens, and F. W. Sheard, in *The Physics and Fabrications of Microstructures and Microdevices*, edited by M. J. Kelly and C. Weisbuch, Springer Proceedings in Physics Vol. 13 (Springer, New York) p. 343.
- [10] A. Zaslavsky, Y. Yuan, P. Li, D. C. Tsui, M. Santos, and M. Shayegan, Phys. Rev. B **42** 1374 (1990).
- [11] K.-M. Hung and G. Y. Wu, Phys. Rev. B **45** 3461 (1992).
- [12] K. Suizu and S. Narita, Phys. Letters **43A**, 353 (1973).
- [13] A. V. Germanenko, V. V. Kruzhaev, G.M. Minkov, E. L. Rumyantsev, and O. E. Rut, Semicond. Sci. Technol. **8**, 383 (1993).
- [14] D. Agassi, Phys. Rev. B **49**, 10393 (1994).

- [15] A. V. Germanenko, G.M. Minkov, E. L. Rumyantsev, and O. E. Rut, *Semicond. Sci. Technol.* **8**, 388 (1993).
- [16] G. M. Minkov, A. V. Germanenko, V. A. Larionova, and O. E. Rut, *Phys. Rev. B* **54**, 1841 (1996).
- [17] G. M. Minkov, A. V. Germanenko, V. A. Larionova, and O. E. Rut, *Semicond. Sci. Technol.* **10**, 1578 (1995).
- [18] D. C. Tsui, *Phys. Rev.* **4**, 1438 (1971).
- [19] L. P. Zverev, V. V. Kruzhaev, G. M. Minkov, and O. E. Rut, *Zh. Eksp. Teor. Fiz.* **80**, 1163 (1981) [*Sov. Phys. JETP* **53**, 595 (1981)]
- [20] Pawel Sobkowicz, *Semicond. Sci. Technol.* **5**, 183 (1990).
- [21] J. C. P. Miller, in *Handbook of Mathematical Functions*, edited by M. Abramowitz and I. A. Stegun (National Bureau of Standards, Washington, DC, 1964) Chap. 13.

## FIGURES

FIG. 1. Energy diagram of metal – insulator – semiconductor structure.  $E_c$  and  $E_v$  are the energies of the edges of conduction and valence bands, respectively.

FIG. 2. Oscillations of tunneling conductivity in a magnetic field at  $V = 130$  mV for various magnetic field orientations for structures I (a) and II (b).

FIG. 3. The bias dependences of tunneling conductivity in magnetic field 4 T for structures I (a) and II (b) for two orientations of magnetic field.

FIG. 4. The model of the energy structure of insulator – semiconductor boundary used for calculations.

FIG. 5. The  $x_0$  dependences of the energy of the Landau sublevels in vicinity of the boundary. The parameters used are given in the text,  $B = 4$  T.

FIG. 6. The  $x_0$  dependences of  $(\hat{v}\Psi)^2$  for  $a_1$  and  $b_1$  Landau sublevels calculated with the same parameters as in Fig. 5,  $B = 4$  T.

FIG. 7. The contributions to the tunneling conductivity of various Landau levels,  $B = 4$  T.

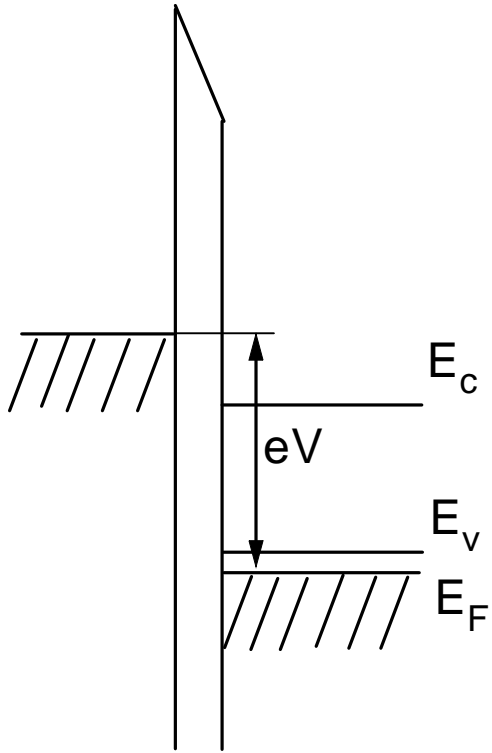
FIG. 8. The oscillatory part of the tunneling conductivity calculated for two orientations of magnetic field,  $B = 4$  T.

FIG. 9. The  $x_0$  dependence of the energy of  $a_1$  and  $b_1$  Landau sublevels calculated for three values of the surface potential.

FIG. 10. Oscillatory part of the tunneling conductivity for three values of the surface potential.

FIG. 11. The fine structure of the tunneling conductivity oscillations in tilted magnetic field for tunnel structure based on p-Hg<sub>1-x</sub>Cd<sub>x</sub>Te with  $E_g = 20$  meV.  $B = 5.5$  T

metal oxide p-HgCdTe



0

2

4

6

8

10



